

DEVELOPMENT OF A REPLACEMENT FOR THE LONG RADIAL PROBE IN THE RING CYCLOTRON

R. Dölling[†], M. Rohrer, G. Gamma, R. Senn, P. Rüttimann, V. Ovinnikov
Paul Scherrer Institut, 5232 Villigen PSI, Switzerland

Abstract

The long radial probe in PSI's Ring cyclotron delivers a radial pattern of all but the first few turns. In recent years, the measurement has been plagued by artefacts and mechanical problems. We report here on the development of a replacement, which should also provide a more flexible basis for extended measurement capabilities.

INTRODUCTION

In 1993 the actual long radial probe RRL1 was installed in the ring cyclotron [1]. It replaced a multi-finger probe operated since 1974 [2], which covered the turns from 110 MeV to 590 MeV at low beam currents.

The almost 3 m long probe is parked in a separately supported chamber connected to an 'intermediate sector' between two of the eight sector magnets. When moved by a wire rope into the cyclotron (Fig. 1), the forks upper and lower trolleys have to transfer from outer to inner rails over a gap of ~5 cm required by the vacuum valve. By using a 33 μm vertical carbon fibre, the radial profile of all but ~6 innermost turns can be measured at full beam current up to 2.4 mA. The probe wire is biased to +60 V in order to suppress thermionic electrons at lower beam energies [3] and to decrease artefacts. From 2002 - 2009, upper and lower fingers from 100 μm SiC, extending vertically until 1 mm



Figure 1: Actual probe fully inserted. The last trolley to the left (not shown) which combines upper and lower arm of the fork stays in the outer chamber. Some of the seven fixtures of the rails are visible.

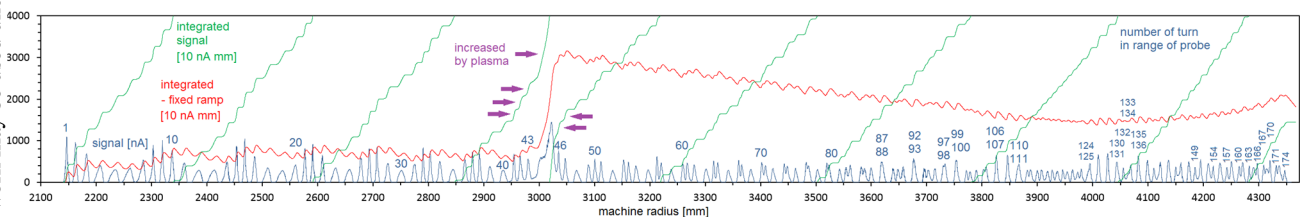


Figure 2: A nicer example of a measurement taken at a beam current of 2200 μA . It is affected by plasma only in a narrow range. A day later, the maximum disturbance was 30 times larger and affected many more turns. With the beam switched off but RF still on, the artefact from the plasma cloud decays within seconds.

[†] rudolf.doelling@psi.ch

Content from this work may be used under the terms of the CC BY 3.0 licence (© 2019). Any distribution of this work must maintain attribution to the author(s), title of the work, publisher, and DOI

BASIC MECHANICAL SETUP

The foreseen probe arrangement is depicted in Fig. 3. A 3.1 m long carrier made of aluminium is rolled from the service chamber into the intermediate sector chamber by a gear operated manually from outside. It will be retracted only for service or repair. The lower and the upper traverse of the carrier are connected at both ends, with the aperture including all turns (Fig. 4). The C-clamp is shaped to fit in the narrow space besides the inflector septum EIC [5]. Suspension by the wheels at both ends of the carrier provides a decoupling of the carrier position from the ‘breathing’ of the vacuum chamber.

On both sides of each traverse, a trolley guided by rails can be moved by a motor via a perforated metal belt driven

by toothed pulleys (Fig. 5) [6]. At one side, upper and lower trolley are moved synchronously by a single motor which drives the pulleys via gear wheels. This allows, e.g., the radial movement of vertical and diagonal carbon fibres in the midplane. Drag chains support the cabling from service chamber to carrier and from traverse to trolley (Fig. 6).

Although located relatively far away from the acceleration cavities, RF stray fields may have an impact to carrier and probe. 40 contact springs provide the grounding of the carrier at several points at ceiling and bottom of the intermediate sector chamber. Carrier temperature will be measured by thermocouples.

Carrier mechanics can be accessed by removing the large flanges. It can be also removed from the vault together with the service chamber by using the vault internal crane.

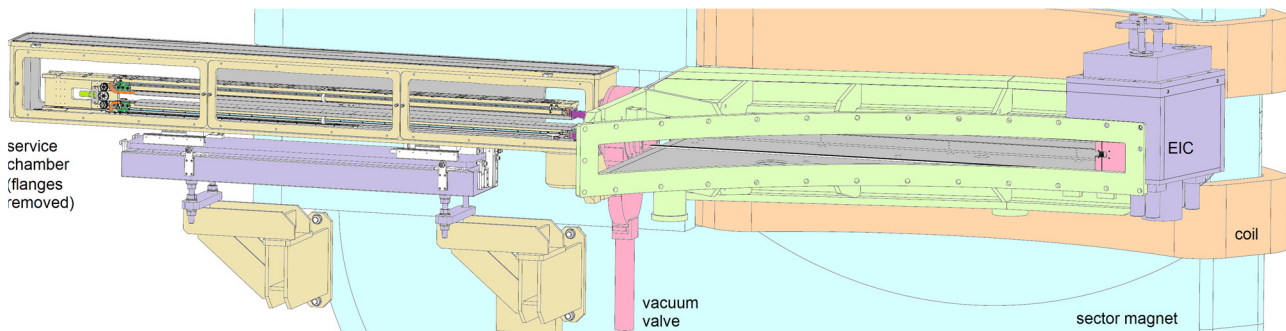


Figure 3: Foreseen arrangement at intermediate sector vacuum chamber. Carrier retracted to service chamber.

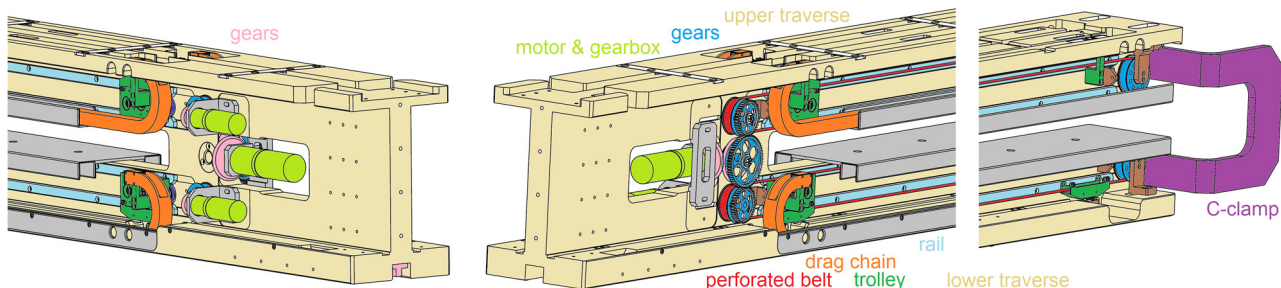


Figure 4: Carrier with drive mechanics. The trolleys carry probe wires, fingers or other sensor.



Figure 5: Test setup with motor, drive belt and an earlier version of drag chain installed.

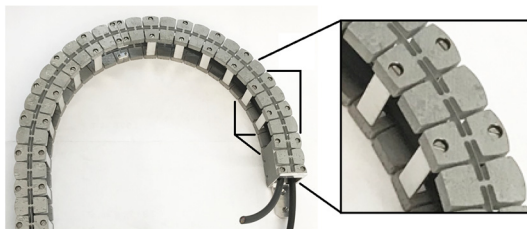


Figure 6: Vacuum compatible aluminium drag chain. Flexor hinges are cut by water jet. The thin fillet is only 0.25 mm wide. Mean radius in operation 34 mm.

COMPONENT TESTS

Shielded Kapton or PEEK insulated cables [7, 8] are well suited for vacuum environments and probably sufficiently radiation hard for the given location, although in the foreseen configuration, the cables stay permanently inside the cyclotron. However, the internal cables must also be well shielded, microphonic noise from the cable movement must be low and cables must survive repeated bending.

Currently we are evaluating these aspects for several cables in the lab. This includes a low-noise coax cable similar to the actually installed ones, coax cables designed for vacuum, as well as individual unshielded Kapton insulated wires combined in a braid with no outer jacket.

Microphonics were roughly tested by placing the cable into the 1.4 m long drag chain to a trolley and moving the trolley with 20 mm/s along 2.5 m forth and back, while injecting 920 pA DC current close to the LogIV [9] logarithmic amplifier module, which was coupled to the fixed

Content from this work may be used under the terms of the CC BY 3.0 licence (© 2019). Any distribution of this work must maintain attribution to the author(s), title of the work, publisher, and DOI

cable end to detect the signal current. An effect of electromagnetic interference from the motor cable was excluded by repeating the same with the tested cable laid closely besides the drag chain. With the low-noise cable, no effect of movement was detected, while for the dedicated vacuum cables the noise level increased quite differently (Table 1). We have to keep in mind that the performance may be different in the real environment or after extensive use or with a bias voltage applied to the wire.

The quality of the cable shield will be tested by placing the cable in a metal tube to which a ± 10 V 1 kHz rectangular signal will be applied by a voltage generator. Tests of the mechanical life time of the cable in the drag chain are also pending.

Table 1: Microphonic Noise in Moving Drag Chain

	type	diam. [mm]	noise [pA _{rms}] at 20 ms/sample integration time
Huber & Suhner G_01130_HT-03	low noise	3.2	~1.4*
VACOM KAP-LCOAX50-AWG26	coax (vacuum)	2.3	~21
VACOM KAP-LCOAX50-AWG30		1.7	~33
Allectra 311-KAP50-RAD		2.3	~76
Allectra 311-KAPM-060-COAX		1.4	~2.8
Allectra 310-PEEK50-TRIAx (shields combined)**		2.7	~2.4
3x Kapton AWG26 (within Allectra 316-BRAID3)	shielded	2.6	~8
4x Kapton AWG26 (within Allectra 316-BRAID4)	multi-wire	2.8	~6
4x Kapton AWG30 (within Allectra 316-BRAID4)	(vacuum)	2.6	~8

Outgassing rates for ~3 m long cable samples were determined, with a connector attached. Differences of about a factor of 10 were observed (Fig. 7). With the dedicated vacuum cables, mainly desorption of water and air was observed. With the low-noise cables the amount of hydrocarbons of 40 to 100 atomic mass units, probably softeners, was larger by a factor of ~40.

Synthetic drag chains were also strongly outgassing. In this aspect, the in-house developed all-metal drag chain is a clear improvement. An endurance tests was performed with a shorter piece of chain at the design radius of 34 mm, using a pressured air actuator. After 2000 cycles no apparent damage was observed. This has to be repeated with the full length and cables inside.

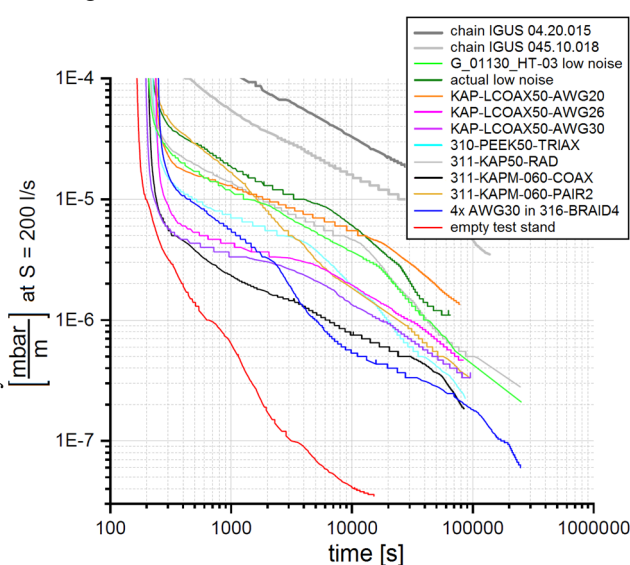


Figure 7: Outgassing rates of cables and drag chains.

While the solutions for the drag chain as well as the non-magnetic and radiation hard materials seem satisfactory, we are still looking for improvements with the cables.

OPTIONAL EXTENDED CAPABILITIES

A 2D-scan of the beam halo could be provided by small ionization chambers at the probe head, moved vertically towards the beam core until a certain signal level is reached (Fig. 8). Beam fractions of the order of 0.1 nA to 1000 nA, limited by background radiation respectively saturation and heating, should be detectable. In the beam lines, a comparable dynamic range could also be delivered by halo monitors, and is already available, however only with little spatial resolution, from beam loss monitors.

Mutual collision by beam protons do not lead to a significant loss of information on the 6-dimensional beam distribution, since the relaxation time of the 'non-neutral plasma' exceeds the duration of the transport through the facility. Also, collisions with the residual gas are not significant in this respect. With this, it seems unlikely that the observation of the beam halo down to fractions of 10^{-7} of the full beam current, over some 170 turns, would not reveal information on the beam distribution, which could be used to better understand beam losses. To a degree, this may allow to design countermeasures, which help to lower activation of machine components. Combination with detailed beam dynamics simulations [10-12, and Refs. in 11, 13] may even allow a prediction of beam losses. However, it is discussed controversially, if this will be ever possible at the limited precision of the available field maps of the magnetic elements and RF cavities which determine the beam transport.

Whether this or other optional probe equipment is to be realized will depend on the future strategy for accelerator development, directed at reducing beam losses, and in general. This applies also to dedicated beam dynamics studies, developments to OPAL [14, 15] as a tool for detailed beam dynamic simulations, as well as to other beam diagnostics systems that deliver the corresponding detailed information, as, e.g., 4-dimensional emittance measurement [13] or bunch-shape monitors [3].

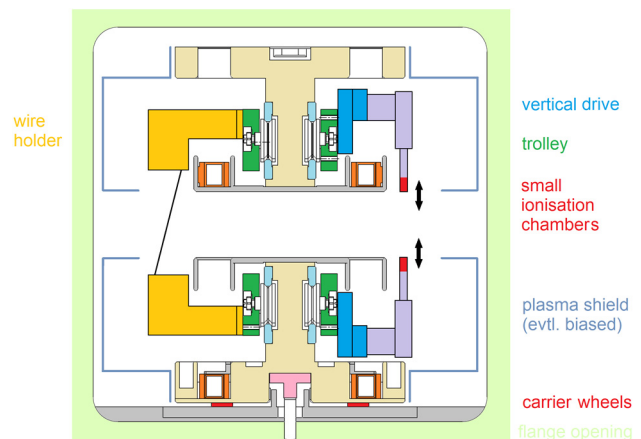


Figure 8: A possible extended configuration of probe heads (schematic, beam from left to right).

OUTLOOK

Delivery of the service chamber is projected for spring 2020, followed by completion of the setup and in-vacuum lab testing of the mechanics. We intend to install in the cyclotron first a basic probe configuration with three carbon wires. Later, shielding electrodes may be added (Fig. 8), which could be biased to ± 100 V and, hopefully, prevent disturbances by plasma clouds.

AUTHOR CONTRIBUTIONS

RD specified the physics layout, guided the development and wrote the paper. MR developed the mechanics concept and detailed layout and oversaw fabrication. RD and RS contributed to the design. RS mounted the mechanical setup and run the cable tests together with GG, who also provided testing software and connector solutions. PR contributed the outgassing tests and its interpretation. VO and GG provided hardware and software for motor tests.

REFERENCES

- [1] L. Rezzonico *et al.*, “Diagnostics for high intensity beams”, in *Proc. BIW'94*, Vancouver, BC, Canada, Oct. 1994, *AIP Conf. Proc.*, vol. 333, pp. 398-494, 1995.
- [2] M. Olivo, “Beam diagnostic equipment for cyclotrons”, in *Proc. Cyclotrons'75*, Zurich, Switzerland, Aug. 1975, paper E-01, pp. 331-340.
- [3] R. Dölling, “Bunch-shape measurements at PSI's high-power cyclotrons and proton beam lines”, in *Proc. Cyclotrons'13*, Vancouver, BC, Canada, Sep. 2013, paper TU3PB01, pp. 257-261.
- [4] D. Goetz *et al.*, “Disturbance effects caused by RF power leaking out from cavities in the PSI ring cyclotron”, in *Proc. Cyclotrons'10*, Lanzhou, China, Sep. 2010, paper WEM2CCO03, pp. 341-343.
- [5] R. Dölling and J. Brutscher, “Fast recharging of electrostatic injection or extraction septa”, presented at the Cyclotrons'19, Cape Town, South Africa, Sep. 2019, paper MOP025, this conference.
- [6] Belt Technologies, Inc., www.belttechnologies.com
- [7] allecra, www.allecra.com
- [8] VACOM, www.vacom.de
- [9] P. A. Duperrex *et al.*, “Latest diagnostic electronics development for the Proscan proton accelerator”, in *Proc. BIW'04*, Knoxville, TN, USA, May 2004, *AIP Conf. Proc.*, vol. 732, pp. 268-275, 2004.
- [10] A. Adelman *et al.*, “Precise simulations of high-intensity cyclotrons”, Paul Scherrer Institute, Villigen, Switzerland, Scientific Report 2010, pp. 54-55.
- [11] M. Frey *et al.*, “Matching of turn pattern measurements for cyclotrons using multiobjective optimization”, *Phys. Rev. Accel. Beams*, vol. 22, p. 064602, Jun. 2019.
doi:10.1103/PhysRevAccelBeams.22.064602
- [12] Y. J. Bi *et al.*, “Towards quantitative simulations of high power proton cyclotrons”, *Phys. Rev. ST Accel. Beams*, vol. 14, p. 054402, May 2011,
doi:10.1103/PhysRevSTAB.14.054402
- [13] R. Dölling and M. Rohrer, “A 4D emittance measurement device for the 870 keV HIPA injection line”, in *Proc. HB'18*, Daejeon, Korea, Jun. 2018, pp. 329-333.
doi:10.18429/JACoW-HB2018-WEP2P0030
- [14] <https://amas.web.psi.ch/>
- [15] A. Adelman *et al.*, “OPAL a versatile tool for charged particle accelerator simulations”, May 2019.
arXiv:1905.06654